Volume 23, No 4 | International Journal of Radiation Research, October 2025

# *In vitro* radiosensitivity of hepatoblastoma cell line huh-6

**L. Xu[1] and Q. Ge[2*]**

[1]*Cancer Research Center Nantong, Affiliated Tumor Hospital of Nantong University, and Medical School of Nantong University, Nantong, China*

[2]*Department of Radiation Oncology, Nantong Tumor Hospital, Affiliated Tumor Hospital of Nantong University, Nantong, China*

► ***Original article***

***Corresponding author:***
*Qin Ge, M.D.,*
***E-mail:*** *geqin.kelley@163.com*

**Received:** June 2024
**Final revised:** February 2025
**Accepted:** April 2025

***Int. J. Radiat. Res., October 2025; 23(4): 895-900***

**DOI:** 10.61186/ijrr.23.4.9

***Keywords:*** *Hepatoblastoma, radiosensitivity, Huh-6 cell line, in vitro.*

## ABSTRACT

***Background:*** As the predominant malignant embryonal liver tumor in children, hepatoblastoma (HB) demonstrates rising incidence rates. While surgical resection and chemotherapy remain primary treatments, radiation therapy emerges as a potential adjuvant option for refractory cases. However, clinical evidence supporting its application remains scarce. To address this knowledge gap, we investigated the radiobiological response of HB cell line Huh-6 through systematic *in vitro* analyses. ***Materials and Methods:*** The proliferation, morphology change, cell apoptosis and cell cycle of Huh-6 cells received gradient X-ray irradiation were systemically conducted with CCK-8 assay, microscopy, Annexin V/7-ADD and PI single staining, respectively. ***Results:*** Irradiation induced dose-dependent suppression of Huh-6 cell proliferation. Morphological assessment demonstrated escalating cytopathic effects with increasing radiation doses, characterized by cytoplasmic vacuolization in the early stage progressing to membrane disintegration and cytosolic debris formation in morphologically aberrant cells during the late stage. Cell apoptosis was enhanced with the increment of irradiation dose. The percentage of cells arrested in G2/M phase increased and meanwhile the proportion of cells in G0/G1 phase decreased with the rising dose gradient. ***Conclusion:*** Our findings demonstrate marked radiosensitivity in Huh-6 cells characterized by dose-responsive growth inhibition, cell apoptosis and cell morphological changes. These experimental results provide preliminary biological validation for considering radiotherapy in HB management protocols, particularly for treatment-resistant cases.

## INTRODUCTION

Hepatoblastoma (HB), accounting for approximately 80% of pediatric malignant liver tumors, is a rare malignancy with an annual incidence of 2 per million children [1-3]. Despite its rarity (<1% of pediatric cancers), epidemiological trends reveal a rising incidence of 1.2-1.5 cases per million annually, potentially linked to increasing survival rates of very low birth weight infants-a known risk factor. Over 90% of cases occur in children under five years old [4]. While multidisciplinary advances have improved five-year survival rates to 80%, therapeutic challenges persist for unresectable tumors present in half of patients at diagnosis [5]. Current protocols prioritize surgical resection or liver transplantation as curative options, supplemented by neoadjuvant chemotherapy to downsize tumors for subsequent surgery [6]. However, chemotherapy-associated toxicity and drug resistance remain significant limitations.

Radiation therapy (RT), utilized in 50% of cancer patients and contributing to 40% of curative treatments [7, 8], has historically been restricted in HB management due to hepatic radiation sensitivity and limited clinical evidence [9-11]. Technological advancements in precision dose delivery and tumor targeting now enable reduced collateral damage to healthy tissues [10, 12]. Emerging data from the International Society of Pediatric Oncology (SIOP) liver tumor study group and clinical reports suggest RT's potential for unresectable tumors or residual lesions <2 cm post-surgery [13], positioning it as a viable salvage or adjuvant therapy[14].

To assess the potential of RT in HB management, we investigated the radiosensitivity of Huh-6 cells- a widely utilized drug-resistant HB model in preclinical research. Cellular proliferation, morphological alterations, and apoptosis were quantitatively analyzed following exposure to graded RT doses. Previous studies focused on therapeutic agents and surgery to combat HB [15, 16]. This systematic evaluation aims to establish a standardized workflow for radiosensitivity research in cell lines while informing optimized RT protocols for HB clinical translation. We enriched the fundamental knowledge of the radiosensitivity of HB, guiding the design of a better therapeutic regimen in HB**.** This is also the first report describing radiosensitivity in HB cell line Huh-6 *in vitro*.



[ DOI: 10.61186/ijrr.23.4.9 ]

## MATERIALS AND METHODS

### *Materials and Reagents*

Dulbecco's Modified Eagle Medium (DMEM) medium (high glucose), FBS, penicillin/streptomycin, and 0.25% Trypsin-EDTA were from Invitrogen (CA, USA), Cell Counting Kit (CCK)-8 kit was from Beyotime (Nanjing, China), Annexin V-PE/7-ADD kit was from KeyGEN BioTECH (Nanjing, China). The HB cell line Huh-6 used in this study was sourced from Cell Bank (Chinese Academy of Sciences, Shanghai, China).

### *Cell culturing and irradiation*

Huh-6 cells were cultured in DMEM medium (high glucose) containing 1% penicillin/streptomycin and 10% FBS in a humidified incubator with 5% of $CO_2$. Before receiving irradiation, Huh-6 cells were digested with 0.25% Trypsin-EDTA and pipetted into single cells. Cells were then counted by TC20™ Automated Cell Counter (BioRad, USA) and $5\times10^5$ cells were seeded into T25 flasks supplemented with 5 ml fresh DMEM medium, subsequently cultured in the incubator overnight till the logarithmic phase. The above cells were then randomly divided into five groups with three flasks of cells in each group. Each group was exposed to a series of irradiation doses 0, 1, 2, 4, and 8 Gy, respectively. X-ray equipment (Varian 2100CD) was used to irradiate the Huh-6 cells with various doses for 6MV X-ray (Dose rate 200 cGy/min, field size 10×10 cm, SSD=100 cm).

### *Cell proliferation by CCK-8 assay*

Two hours after irradiation, the cell culture was centrifuged at 200 g for 5 min and the supernatant was discarded. Huh-6 cells were digested to single cell suspension by 0.25% Trypsin-EDTA after that. After gently pipetting, the single cell suspension was carefully counted and then adjusted to a density of $2\times10^4$ /ml. 100 µl of this density-adjusted cell suspension (2000 cells) was transferred into each well on a 96-well plate and then cultured in the incubator under the same conditions as mentioned above. For each experimental group, five repeated wells were conducted. CCK-8 kit was applied to check the proliferation of cells in each well at 1, 3, 5, 7, and 14 days after irradiation, following the manufacturer's instruction. CCK-8 reagent was gently loaded into the medium in each well except for the blank control, and then cultured in the incubator for 2 hours. The OD450 for each well was measured by a plate reader (EON, BioTek, USA). The indices used for evaluating the proliferation were calculated as follows: Cell survival fraction (SF) (%) = $(OD_{exp} - OD_{basal}) / (OD_{ctrl} - OD_{basal}) \times100\%$, cell inhibitory fraction (%) = $(OD_{ctrl} - OD_{exp}) / (OD_{ctrl} - OD_{basal}) \times100\%$. $OD_{exp}$, $OD_{ctrl}$ and $OD_{basal}$ represented the OD450 of experimental groups (1, 2, 4, 8 Gy), control group (0 Gy), and culture medium only respectively.

### *Cell morphological change by microscopy*

Huh-6 cell morphology was monitored by an inverted microscopy (IX-71, Olympus, Japan) at 1, 2, 3, 5, and 14 days after the irradiation with various doses. Pictures were captured with the controller software coupled with the equipment.

### *Cell cycle and apoptosis analysis by FACS*

24, 48, and 72 hours after the irradiation, Huh-6 cells were harvested and filtered through a 70 µm cell strainer to get rid of any aggregates. The suspension was centrifuged at 200 x g for 5 min. The cell pellet was washed with cold PBS twice and re-suspended with 70% pre-chilled ethanol and kept at 4°C overnight to get fixed. The fixed cells were centrifuged at 200x g for 5 min and washed with PBS once, and re-suspended with 500ul PBS containing 50 µg/ml PI and 100 µg/ml RNase A. The PI Staining process was conducted at 4°C for 0.5h. The PI-stained cells were analyzed by Fluorescence-activated cell sorting, FACS (NovoCyte, ACEA, USA) immediately after the staining was done. In the controller software NovoExpress 1.0 (ACEA, USA), the parameters were set as follows: flow rate: 66 µl/min, event count: 30,000, 488 nm laser power: 20mW, PMT voltages for BL1(FITC), BL2 (PE), BL4 (PerCP), BL5 (PE-Cy7) were 448, 386, 483, 433, respectively, threshold for FSC was set at larger than 10,000. In the FSC-H and SSC-H dot plots, all the cells except the small debris shown in the lower left corner were selected in the first gate for the following analysis. In the FSC-H and FSC-A dot plots, the cells shown in the diagonal line were selected in the second gate for the following analysis, to remove the cell aggregates. BL2 PMT channel was used to detect the PI fluorescence. The cell cycle result was automatically analyzed in a cell cycle plot by the software NovoExpress 1.0 after running each sample.

Cells for Annexin V-PE/7-ADD staining were harvested at the same time points and with the same methods mentioned above and then stained with Annexin V-PE/7-ADD following the manufacturer's instruction. Briefly, $2\times10^5$ Huh-6 cells were pooled and washed with PBS twice, and re-suspended with 50 µl Binding Buffer supplemented with 5 µl 7-ADD staining solution, incubated at room temperature for 10 min avoiding light exposure. After that, 450 µl Binding Buffer and 1 µl Annexin V-PE/7-ADD staining solution were added in succession, followed by incubation in the dark. The cell samples were subsequently analyzed by FACS to check the apoptosis within one hour. BL2 and BL4 PMT channels were used to detect the Annexin V-PE and 7 -ADD fluorescence respectively. The compensation between BL2 and BL4 was set to BL4-18% BL2 and BL2-0.95% BL4. Other parameter settings were kept the same as mentioned above for PI staining.



[ DOI: 10.61186/ijrr.23.4.9 ]

### *Statistics analysis*

Two-way ANOVA analysis was conducted for the cell proliferation data. Mann-Whitney test was used to compare the difference of cell apoptosis percentage between groups. The percentage of cells at different cell cycle stages among individual groups was analyzed by two-tailed, unpaired Student's t-test. Experimental data were analyzed by SPSS (SPSS 22, Chicago, USA). *P* values <0.05 were considered to be statistically significant.

## RESULTS

### *Irradiated Huh-6 cells showed impaired proliferation*

In general, the irradiation significantly inhibited the proliferation of Huh-6 cells and the inhibition efficiency was positively correlated with the irradiation dose (figure 1). The irradiated cells had a similar growth curve to the normal cells, characterized by rapid proliferation in the first 3 days post irradiation and declined proliferating speed thereafter. However, the proliferation of irradiated cells was significantly impaired and the growth rate decreased with the increase of irradiation dose. For all the cells that received different doses of irradiation, their cell survival fractions decreased sharply within 5 days post irradiation but had a rebound on day 7 and stayed relatively stable until experimental termination, except the 8 Gy group which had no rebound but gradually reduced cell survival fraction during the entire experiment.

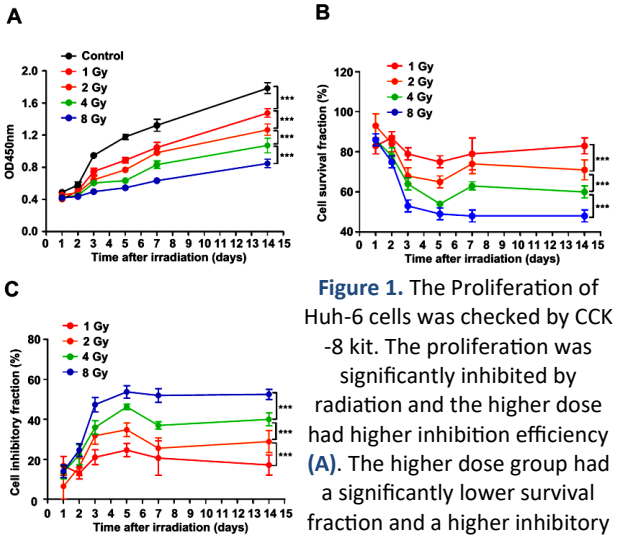


**Figure 1.** The Proliferation of Huh-6 cells was checked by CCK -8 kit. The proliferation was significantly inhibited by radiation and the higher dose had higher inhibition efficiency **(A)**. The higher dose group had a significantly lower survival fraction and a higher inhibitory fraction **(B and C)**. ***: p<0.001.

### *The morphology of Huh-6 cells altered after irradiation*

The results (figure 2) illustrated that the percentage of deformed cells increased with the rise of irradiation dose during the entire experiment period. At the early stage after irradiation, apoptotic cells marked by plenty of bubbles in the cytosol accounted for the majority of the deformed cells. While dead cells featured with rounded or non-regular shape, much debris in the cytosol and floating in the medium comprised the most proportion of the deformed cells at the later stage. These changes were more remarkable in the higher dose groups and the change extent increased with time. On the contrary, no or little such morphological changes were observed in the control or low dose (1 Gy) group.

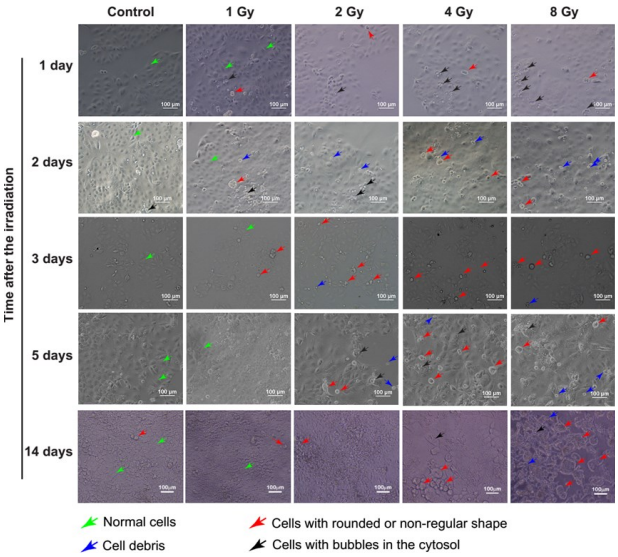


**Figure 2.** Morphological changes of Huh-6 cells post irradiation by inverted microscopy. The higher dose group showed a higher percentage of deformed cells characterized by plenty of bubbles in the cytosol at the early stage, and dead cells featured rounded or non-regular shape and debris in the cytosol. The change extent increased over time. The scale bar represents 100 μm.

### *The apoptosis of Huh-6 cells correlated with the dose of irradiation*

The results of FACS after standard Annexin V/7-ADD staining revealed that with the increase of radiation dose, more cells were located in the Annexin V-PE+/7-ADD- and Annexin V-PE+/7-ADD+ quadrants, which represented the early and late apoptotic cells respectively (figure 3). The apoptosis was enhanced with the increment of the irradiation dose. It was also reasonable to find that the apoptosis gradually augmented over time after irradiation. These findings were further confirmed by PI single staining and cell cycle analysis results (table 1). An increasing number of cells were arrested in G2/M phase with the increasing irradiation dose, which showed a dose-dependent feature. Meanwhile, the cell number in G0/G1 phase decreased with the rising dose gradient, which indicated that the DNA synthesis was inhibited before S phase. The cell cycle arrest reached its peak 48 hours after the irradiation, then it was partially relieved and allowed the cells to return back to the normal cell cycle or directly turn into apoptosis. Generally speaking, these results indicated that the apoptosis of Huh-6 cells was



[ DOI: 10.61186/ijrr.23.4.9 ]

correlated with the dose of irradiation received.

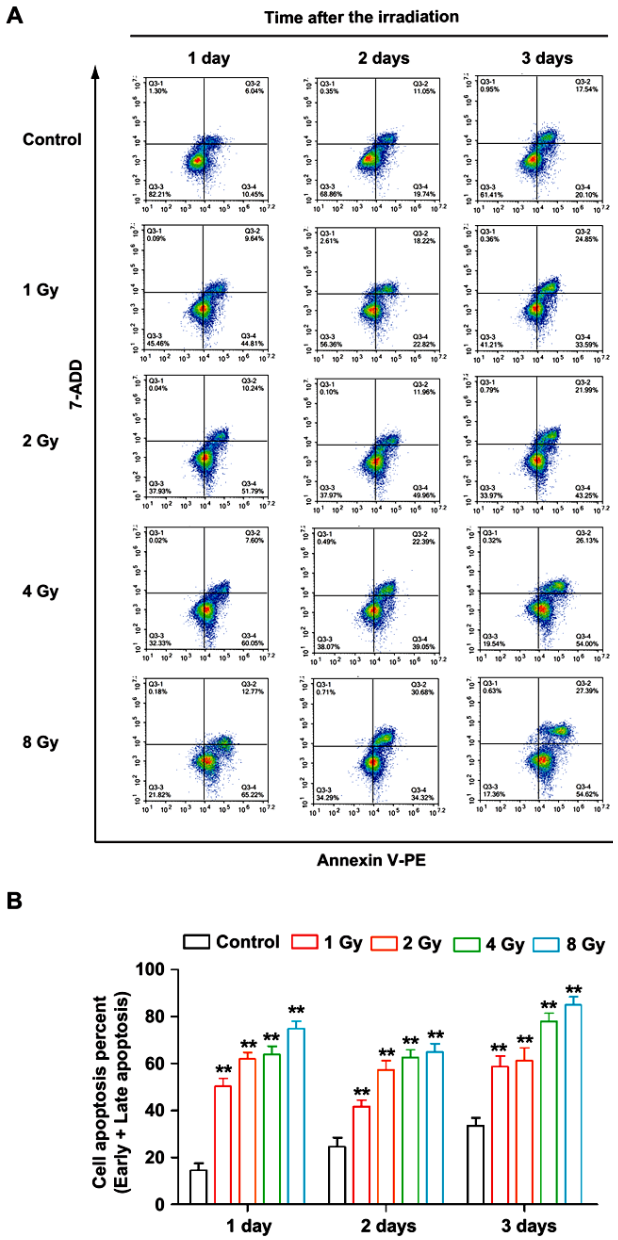


**Figure 3.** Apoptosis of Huh-6 cells checked by FACS with Annexin V-PE/7-ADD staining. With the increase of radiation dose, more cells were located in the Annexin V-PE+/7-ADD- and Annexin V-PE+/7-ADD+ quadrants, which represent the early and late apoptotic cells respectively **(A)**. The higher dose group had a higher percentage of cells at the early or late apoptosis stage **(B)**. **: p<0.01.

## DISCUSSION

RT exerts its cytotoxic effects primarily by exploiting the accelerated mitotic rate of malignant cells, which limits DNA damage repair during irradiation and culminates in apoptotic cell death through cumulative genomic instability [17]. Clinically, RT serves as a neoadjuvant or adjuvant modality to debulk tumors and eliminate residual micrometastases, enhancing surgical outcomes. Notably, *in vitro* radiosensitivity assays using human tumor cell lines have demonstrated predictive value for clinical radiocurability, underscoring their utility in personalized RT planning [18]. Systematic evaluation of radiation responsiveness in preclinical models further enables dose fractionation optimization and temporal sequencing adjustments, maximizing therapeutic efficacy while sparing normal tissues.

**Table1.** Percentage of Huh-6 cells at G0/G1, S, and G2/M stages at different time points after irradiation.

| Time | Dose | Cell cycle stage | | |
|---|---|---|---|---|
| | | G0/G1 | S | G2/M |
| 24 h | 0 Gy | 46.53±1.04 | 35.33±0.78 | 18.14±1.32 |
| | 1 Gy | 46.80±1.24 | 31.74±0.87** | 21.46±1.53* |
| | 2 Gy | 44.60±1.62 | 27.86±1.15*** | 27.54±1.33*** |
| | 4 Gy | 41.07±1.33** | 25.77±1.09*** | 33.16±1.52*** |
| | 8 Gy | 34.01±1.11*** | 23.19±0.83*** | 42.80±1.62*** |
| 48 h | 0 Gy | 42.72±1.52 | 36.39±1.31 | 20.35±1.24 |
| | 1 Gy | 39.11±0.83* | 37.34±0.99 | 23.55±0.96* |
| | 2 Gy | 32.28±1.34*** | 39.63±1.52 | 28.09±0.82*** |
| | 4 Gy | 28.30±1.32*** | 35.92±0.73 | 35.78±1.27*** |
| | 8 Gy | 25.82±1.17*** | 25.62±1.41*** | 48.56±1.33*** |
| 72 h | 0 Gy | 51.84±1.63 | 41.75±1.12 | 6.41±0.69 |
| | 1 Gy | 48.13±1.54* | 34.75±0.74*** | 17.12±1.41*** |
| | 2 Gy | 44.48±0.94** | 29.39±0.84*** | 26.13±0.91*** |
| | 4 Gy | 37.23±1.28*** | 34.11±1.14** | 28.66±1.16*** |
| | 8 Gy | 35.72±1.42*** | 29.02±1.27*** | 35.26±1.58*** |

*: p<0.05, **: p<0.01, ***: p<0.001, when compared to the control group (0 Gy).

Our study revealed radiation-induced, dose-dependent inhibition of Huh-6 cell proliferation. Notably, while a transient proliferation rebound occurred on day 5, the survival fraction remained consistently suppressed throughout observation. These findings suggest higher radiation doses may optimize HB treatment by maintaining sustained proliferation control. In our study, the proliferation of Huh-6 cells was inhibited by radiation and the inhibition efficiency was positively correlated with the irradiation dose. Notably, the proliferation of Huh -6 cells recovered over time, and a rebound of proliferation was observed on day 5, in which the survival fraction stayed at a lower level and did not show signs of rebound in the whole observation process. This result implied that a higher dose of radiation might be preferable for the HB treatment by providing continuous and stable suppression of tumor cell proliferation.

Beyond merely suppressing cellular proliferation, radiation exerts its therapeutic effects through cell apoptosis, death and redistribution of the cell cycle during the irradiation period are extra crucial factors to consider [14]. Irradiation critically targets into and generate DNA damage, cause cell apoptosis and death, particularly for the active tumor cells [19]. Our investigation revealed that the apoptosis also witnessed dose dependence and gradually augmented over time within 3 days after the irradiation, which is consistent with the cell survival curves. Usually, high-dose radiation is considered to be more efficient than



[ DOI: 10.61186/ijrr.23.4.9 ]

low-dose radiation to induce cell apoptosis as tumor cells may have enough time to repair for dose impairment. Irradiation damage activates the DNA damage response (DDR) kinase signal pathway, resulting in apoptosis, DNA rearrangements, or cell cycle arrests after irradiation. The S phase is a particularly vulnerable period for DNA damage exposure and apoptosis can be preceded by accumulation of cell numbers in the G2/M phase [20, 21].

Our results indicated that the higher dose groups had more cells in the S and G2/M phases, indicating that the cells received higher doses of radiation were more likely to divide with damaged DNA and go through the cycle of cell death. While control cells without irradiation, a higher proportion were arrested G0/G1 phase so that the cell would have enough time for repairment. For the time effect, the cell cycle arrest reached its peak 48 hours after the irradiation, thereafter the arrest was partially relieved or transient, which allowed the cells to return to the normal cell cycle or directly turn to apoptosis. Collectively, the present study is the first to report that the apoptosis of Huh-6 cells was correlated with the dose of irradiation. This property is consistent with previous studies in other tumor cell lines [22, 23].

Besides, the inhibition of proliferation and apoptosis are often accompanied with the changes of cell morphology, which is another important factor for radiotherapy. In this study, less intact cells and more cell debris were witnessed in the post irradiated Huh-6 cells, indicating the increased cell death. And the morphological changes aggravated as the dose and time increased. However, Huh-6 cell line was less considered in previous studies. This may make it difficult to compare our results with other studies.

## CONCLUSION

Our results indicated an obvious sensitivity of Huh-6 cells following impaired cell proliferation, induced cell apoptosis and cell morphological changes, showing the therapeutic potential of precision radiotherapy in HB management. More clinical radiotherapy experiment is also crucial for optimizing the real radiotherapy settings such as single dose or fractionated, dose rate and amount, whether pretreatments needed.

***Acknowledgment*:** None

***Conflict of Interest Statement*:** The authors have no conflicts of interest to disclose.

***Funding*:** The study was funded by the Nantong Municipal science and technology project (2022LZ010) and Nantong City's' 226 'Second Level Talents fund RC202310.

***Authors' contribution*:** All authors participated equally in research and preparation of the manuscript. All authors have ead and agreed submission of the manuscript for publication.

## REFERENCES


1. Cao Y, Wu S, Tang H (2024) An update on diagnosis and treatment of hepatoblastoma. B*iosci Trends, **17**: 445-457.*
2. Guo C, Liu Z, Zhang X, Zhao S, Fan H, Wang H, *et al.* (2025) Global, regional, and national epidemiology of hepatoblastoma in children from 1990 to 2021: a trend analysis. *Hepatol Int, **19**(1): 156-165.*
3. Meyers R, Hiyama E, Czauderna P, Tiao GM (2021) Liver tumors in pediatric patients. *Surg Oncol Clin N Am, **30**: 253-274.*
4. Wu Z, Xia F, Wang W, Zhang K, Fan M, Lin R (2024) Worldwide burden of liver cancer across childhood and adolescence, 2000-2021: a systematic analysis of the global burden of disease study 2021. *EClinicalMedicine, **75**: 102765.*
5. Yang L, Yu Z-Q, Zhang Y-Z, Deng Y-Q, Chen X, Liu H-Y, *et al.* (2025) Global, regional, and national burden of hepatoblastoma, 1990-2021: a systematic analysis of the global burden of disease study 2021. *Int J Surg, **111**(5): 3629-3633.*.
6. Wu PV and Rangaswami A (2022) Current Approaches in hepatoblastoma-new biological insights to inform therapy. *Curr Oncol Rep, **24**: 1209-1218.*
7. Razvi Y, Chan S, Zhang L, Tsao M, Barnes E, Danjoux C, *et al.* (2019) A review of the Rapid Response Radiotherapy Program in patients with advanced cancer referred for palliative radiotherapy over two decades. *Support Care Cancer, **27**: 2131-2134.*
8. Huang Z, Li N, Tang Y, Jin J, Liu W, Xu H, *et al.* (2022) Neoadjuvant radiotherapy for soft tissue sarcoma in China: a preliminary result. *Ann Transl Med, **10**: 452.*
9. Sun D-E and Ye S-Y (2020) Emerging roles of long noncoding RNA regulator of reprogramming in cancer treatment. *Cancer Manag Res, **12**: 6103-6112.*
10. Qi J-S, Wang W-H, Li F-Q (2015) Combination of interventional adenovirus-p53 introduction and ultrasonic irradiation in the treatment of liver cancer. *Oncol Lett, **9**: 1297-1302.*
11. Ma F, Zhang W, Sun X (2024) m6A methylation pattern of SLC7A11 mediates the effects of cinobufagin on hepatocellular carcinoma cell proliferation and radioresistance. *International Journal of Radiation Research, **2**(2: 481-486.*
12. Zhang K, Tao C, Siqin T, Wu J, Rong W (2021) Establishment, validation and evaluation of predictive model for early relapse after R0 resection in hepatocellular carcinoma patients with microvascular invasion. *J Transl Med, **19**: 293.*
13. Leal-Leal CA, Imaz-Olguín V, Robles-Castro J, Shalkow-Klincovstein J, Palacios-Acosta JM (2010) Hepatoblastoma. Clinical experience at a single institution using the Siopel staging system. *Ann Hepatol, **9**: 75-79.*
14. Wang Z-H, Liu Y, Guo J-Q, Liang H-L, Zhi W-W (2024) Research progress in the application of radiotherapy in the treatment of pediatric tumors. *International Journal of Radiation Research, **22**: 65-75.*
15. Lu Z, Xu H, Yu X, Wang Y, Huang L, Jin X, *et al.* (2018) 20(S)-Protopanaxadiol induces apoptosis in human hepatoblastoma HepG2 cells by downregulating the protein kinase B signaling pathway. *Exp Ther Med, **15**: 1277-1284.*
16. Makimoto A, Matsui M, Chin M, Koh K, Tomotsune M, Kaneko T, *et al.* (2019) Magnesium supplementation therapy to prevent cisplatin-induced acute nephrotoxicity in pediatric cancer: A protocol for a randomized phase 2 trial. *Contemp Clin Trials Commun, **16**: 100440.*
17. Pariset E, Bertucci A, Petay M, Malkani S, Lopez Macha A, Paulino Lima IG, *et al.* (2020) DNA damage baseline predicts resilience to space radiation and radiotherapy. *Cell Rep, **33**: 108434.*
18. Qin H, Ke J, Dong S, Li H, Zhu K, Fu S, *et al.* (2022) Effect of thoracic radiotherapy dose on the prognosis of advanced lung adenocarcinoma harboring EGFR mutations. *BMC Cancer, **22**: 1012.*
19. Wang J, Liu J, Wang J, Wang S, Li F, Li R, *et al.* (2022) Identification of proteomic markers for prediction of the response to 5-Fluorouracil based neoadjuvant chemoradiotherapy in locally advanced rectal cancer patients. *Cancer Cell Int, **22**: 117.*
20. Jiang H, Li Q, Chen B, Xi M, Makelike K, Liu S, *et al.* (2023) Phase I study of cisplatin and nanoparticle albumin-bound-paclitaxel combined with concurrent radiotherapy in locally advanced




[ DOI: 10.61186/ijrr.23.4.9 ]

esophageal squamous cell carcinoma. *Cancer Med, 12: 15187-15198*.
21. Hong J-D, Wang X, Peng Y-P, Peng J-H, Wang J, Dong Y-P, *et al.* (2017) Silencing platelet-derived growth factor receptor-β enhances the radiosensitivity of C6 glioma cells in vitro and in vivo. *Oncol Lett, **14**: 329-336*.
22. Zhang A-D, Su X-H, Wang Y-F, Shi G-F, Han C, Zhang N (2021) Predicting the effects of radiotherapy based on diffusion kurtosis imaging in a xenograft mouse model of esophageal carcinoma. *Exp Ther Med, **21**: 327*.
23. Fei Z, Chen T, Qiu X, Chen C (2020) Effect of relevant factors on radiation-induced nasopharyngeal ulcer in patients with primary nasopharyngeal carcinoma treated with intensity-modulated radiation therapy. *Laryngoscope Investig Otolaryngol, **5**: 228-234*.



[ DOI: 10.61186/ijrr.23.4.9 ]